Ann. Geophys., 30, 109–117, 2012
www.ann-geophys.net/30/109/2012/
doi:10.5194/angeo-30-109-2012


Annales Geophysicae

# Electron pitch angle distribution during magnetic reconnection diffusion region observations in the Earth's magnetotail

**A. L. Borg**[1], **M. G. G. T. Taylor**[1], **and J. P. Eastwood**[2]

[1]ESTEC/European Space Agency, Noordwijk, The Netherlands
[2]The Blackett Laboratory, Imperial College London, London SW7 2AZ, UK

*Correspondence to:* A. L. Borg (anette.l.borg@gmail.com)

Received: 20 April 2011 – Revised: 30 November 2011 – Accepted: 2 January 2012 – Published: 13 January 2012

**Abstract.** The Earth's magnetosphere provides an excellent laboratory for magnetic reconnection research. In particular, the magnetotail current sheet that is formed between the interface of the similar Northern and Southern Hemispheres of the magnetotail provides a relatively stable symmetric reconnection configuration that can be used to study basic aspects of the reconnection process. Of particular importance is the manner in which electrons are processed by the reconnection. Simulations and satellite data analyses of the ion diffusion region have suggested that the fluxes of electrons in the inflow regions of reconnection are greater in the directions parallel and anti-parallel to the magnetic field (field-aligned) whereas the electron flux in the outflow region is distributed more isotropically. However, this has only been studied experimentally on a case-by-case basis. In this paper, we investigate this claim by analyzing the degree of bulk electron field alignment in the outflow and inflow regions during encounters of the magnetic reconnection ion diffusion region by the Cluster spacecraft in the years 2001–2006. We demonstrate that while the median electron flux in the inflow region is indeed more field aligned than in the outflow region during some ion diffusion region encounters, the variation of the signature across events is so large that it cannot be said to be a general feature of magnetic reconnection in the Earth's magnetotail.

**Keywords.** Magnetospheric physics (Magnetotail) – Space plasma physics (Magnetic reconnection)

## 1 Introduction

Magnetic reconnection is a plasma process where magnetic energy is converted into particle energy and the magnetic field topology is changed (Vasyliunas, 1975). The process plays a fundamental part in phenomena such as solar flares (Giovanelli, 1946) and magnetospheric substorms (Nagai et al., 2001). Magnetic reconnection in the Earth's magnetotail has been observed by several spacecraft and the observations have addressed many of the predictions found in literature, such as the Hall magnetic field, the Hall electric field and the production of magnetic flux ropes (Fujimoto et al., 1997; Øieroset et al., 2001; Slavin et al., 2003; Borg et al., 2005).

Figure 1 shows a 2-D simplified cartoon of the ion diffusion region of an ongoing symmetric reconnection process in the Earth's magnetotail. Magnetic fields of opposite polarity meet and reconnect in the interface between the Northern and Southern Hemispheres. Plasma enters the reconnection process in the inflow regions, which extend outside the diffusion regions of Fig. 1. Outside the diffusion regions, the plasma particles are bound to the magnetic field lines and convecting due to a strong electric field in the Y-direction until they encounter the ion diffusion region. Inside the ion diffusion region the ions become demagnetized while the electrons keep moving with the magnetic field until they encounter the much smaller electron diffusion region. This separation of ion and electron flows inside the ion diffusion region causes the Hall currents and the Hall quadrupole magnetic field. Inside the electron diffusion region the magnetic field lines reconnect and the newly formed field lines move apart in the outflow regions. As these field lines reach the areas outside the diffusion regions, plasma particles are again bound to the rapidly moving field lines causing fast plasma jets moving in

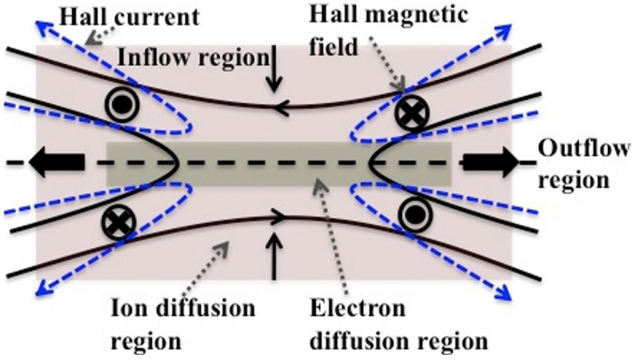


**Fig. 1.** 2-D cartoon of magnetic reconnection, see text for explanations.

opposite directions. In this 2-D image of reconnection, there is a region separating the inflow and outflow regions known as the separatrix. In this paper, the words "inflow region" and "outflow region" will be used to describe only the parts of these regions residing inside the ion diffusion region.

Simulations and analyses of satellite measurements in recent years have suggested that the electron flux in the inflow region is mostly moving parallel and anti-parallel (field aligned) to the magnetic field direction whereas the electrons in the outflow region have a flat-top isotropic distribution due to heating occurring during the reconnection process (Nagai et al., 2001; Egedal et al., 2005; Asano et al., 2008; Chen et al., 2008; Egedal et al., 2010; Le et al., 2010). The reason cited is the conservation of the first adiabatic invariant $\mu = mv_{\perp}^2/(2B)$. In the inflow region, the electrons are moving with the magnetic flux toward the electron diffusion region. During this movement, they experience a decrease in the magnetic field magnitude causing the velocity perpendicular to the magnetic field direction to decrease. In Chen et al. (2008), the difference in electron movement in the inflow and outflow regions is clearly demonstrated using measurements taken by the Cluster satellites during the reconnection event on 1 October 2001. The inflow region electron flux is shown to be mostly field aligned and the outflow electron flux more isotropic.

Whilst considerable progress has been made from the detailed study of individual events, the extent to which such differences in the inflow and outflow regions are a general feature of reconnection is not clear. To address this point, in this paper we investigate the properties of electrons in the inflow and outflow regions during 21 ion diffusion region encounters in the Earth's magnetotail using measurements from the Cluster satellites. The paper is organized as follows: in Sect. 2 the data and data selection are presented, in Sect. 3 the properties of electrons are analyzed before being discussed in detail in Sect. 4. In Sect. 5, the results are summarized.

**Table 1.** Ion diffusion region encounters by the Cluster satellites 2001–2006.

| Event number | Date and time interval |
|---|---|
| 1 | 22 Aug 2001, 09:40:00–10:16:00 |
| 2 | 10 Sep 2001, 07:48:00–08:04:00 |
| 3 | 12 Sep 2001, 13:11:00–13:24:00 |
| 4 | 15 Sep 2001, 05:01:00–05:16:00 |
| 5 | 1 Oct 2001, 09:37:00–10:01:00 |
| 6 | 8 Oct 2001, 12:33:00–13:02:00 |
| 7 | 11 Oct 2001, 03:24:00–03:44:00 |
| 8a | 18 Aug 2002, 17:03:00–17:15:00 |
| 8b | 18 Aug 2002, 17:27:00–17:36:00 |
| 9 | 21 Aug 2002, 07:54:00–08:25:00 |
| 10 | 28 Aug 2002, 10:00:00–10:11:00 |
| 11 | 13 Sep 2002, 18:07:00–18:25:00 |
| 12 | 18 Sep 2002, 12:57:00–13:40:00 |
| 13 | 2 Oct 2002, 21:17:00–21:38:00 |
| 14 | 17 Aug 2003, 16:32:00–17:03:00 |
| 15 | 24 Aug 2003, 18:39:00–19:14:00 |
| 16 | 19 Sep 2003, 23:25:00–23:33:00 |
| 17 | 4 Oct 2003, 06:18:00–06:35:00 |
| 18 | 9 Oct 2003, 02:18:00–02:31:00 |
| 19 | 14 Sep 2004, 23:00:00–23:08:00 |
| 20 | 28 Aug 2005, 23:36:00–23:51:00 |
| 21 | 26 Sep 2005, 09:35:00–09:57:00 |

## 2 Data

The data used in this paper was obtained from the Cluster four-spacecraft mission through the Cluster Active Archive (Laakso et al., 2010). The magnetic field data was provided by the Flux-Gate Magnetometer (FGM) experiment (Balogh et al., 2001) and the ion plasma data were measured by the Cluster Ion Spectrometry (CIS) experiment (Rème et al., 2001). The electron data are from the Plasma Electron and Current Experiment (PEACE) (Johnstone et al., 1997). In the analysis, only the PEACE data points with values above the background electron flux count that were also flagged with quality number 3 or 4 (Good for publication) were used. Both the HEEA (high energy sensor) and the LEEA (low energy sensor) data were included. The electron differential energy flux measurements at spacecraft spin resolution (4 s) are given for 12 pitch angle bins (bin width of 15°) and 44 energy levels (ranging from tens of eV to tens of keV). The pitch angle of a particle is the angle between the direction of motion of the particle and the direction of the magnetic field. To avoid photo electron measurements we consider only electrons at energy levels higher than 70 eV. The PEACE electron moments measured are given at varying time resolution (4–160 s).

The time intervals of interest (the spacecraft observing the magnetic reconnection inflow and outflow regions) were found studying in detail the ion diffusion region encounters on a list of 21 magnetic reconnection encounters by the

Cluster satellites (Table 1). This list of reconnection encounters, covering 2001–2006, was compiled by visual inspection of the data and is a continuation of those presented in Borg (2006). The list also includes those reported by Eastwood et al. (2010). Most of the encounters have previously been studied by other authors. The list reveales a very skewed distribution of ion diffusion region encounters, with most encounters occurring in 2001–2003 and with a sharp drop to 1 identified encounter in 2004 and 2 in 2005. No ion diffusion region encounters were found in the 2006 data. This paucity of encounters after 2005 is thought to be due to a combination of orbit evolution, where Cluster crossed the neutral sheet progressively closer to the Earth each year, and the solar cycle effect on near-Earth magnetotail reconnection location with lower solar activity resulting in an average position further from the Earth (Nagai, 2006).

To identify ion diffusion region encounters in this study the "ideal" 2-D image of reconnection geometry (shown in Fig. 1) was used and it was assumed that the dominant direction of motion of an ion diffusion region across the satellites was in the $\pm X_{\mathrm{GSM}}$ directions. We note that previous studies have used similar criteria (Borg, 2006; Eastwood et al., 2010). The criteria were: (1) High ion velocity ($\sim$200 km s$^{-1}$ or more) with a change of polarity in the ion velocity X component ($V_{\mathrm{x}}$), (2) simultaneous change of polarity in the magnetic field Z component ($B_{\mathrm{z}}$) and (3) presence of the Hall quadrupole magnetic field in the magnetic field Y component ($B_{\mathrm{y}}$) during the ion flows. (4) (1)–(3) should be observed in connection with a Cluster traversal of the magnetotail current sheet (reversal of magnetic field X component ($B_{\mathrm{x}}$)). The outflow regions were then identified as a sub-period of the entire ion diffusion region encounter, specifically the high ion flow velocity regions, matching magnetic Z component and Hall magnetic field. To ensure that only data points from inside the ion diffusion were included, additional critera were added: $E + v_{\mathrm{i}} \times B \neq 0$ and $E_{\mathrm{z}}$ pointing in the direction of the neutral sheet. Low resolution data was a complicating factor in trying to check whether $E + v_{\mathrm{i}} \times B \neq 0$ during short outflow intervals. The resolution of the CIS data, including the ion velocities, is 8 s and the spin resolution of the magnetic and electric field measurements is 4 s. Because of these limitations, only the general trend of the electric field data and $-v_{\mathrm{i}} \times B$ were compared as absolute differences were too sparse.

As far as the authors are aware, a clear definition has not been used for the inflow regions in previous publications. In the current paper we use a combination of data signatures and geometric arguments involving simultaneous multi-spacecraft measurements combined with the constraints given by the simple 2-D picture of reconnection presented in Fig. 1. The inflow region signatures considered were: (1) no observations of high velocity ion outflow, (2) the spacecraft situated inside the ion diffusion region where $E + v_{\mathrm{i}} \times B \neq 0$, (3) no crossing of the neutral sheet (change of $B_{\mathrm{x}}$ polarity) during the time interval and (4) the location of the spacecraft outside of the separatrix region. Another possible inflow signature arises from the fact that the still-magnetized electrons are convecting at the $E \times B$ velocity in the Z direction due to the reconnection electric field $E_{\mathrm{y}}$. Unfortunately the low resolution of the Cluster electron velocity measurements (often at 10s of seconds or more) did not allow any useful comparisons. Spacecraft 2 did provide higher resolution electron moments, but as the CIS experiment does not work on this spacecraft there is no way of determining when it is situated in the outflow and inflow regions. The separatrix region was identified by simultaneous observations of a clear local minimum in the density and a local maximum in the full resolution (0.02 s) electric field (Retinò et al., 2006; Khotyaintsev et al., 2006) during intervals adjacent to outflow region observations. Due to gaps in the density and electric field data, it was not always possible to check both parameters for the separatrix signature and resulted in only one clear separatrix signature being resolved.

The actual search for inflow region observation was conducted as follows: for each ion diffusion region encounter, we searched for time intervals where one or more spacecraft detected inflow signatures while some or all remaining spacecraft were simultaneously sampling an outflow region. We then compared the relative spacecraft positions to the geometric 2-D picture in Fig. 1. A few inflow intervals were also identified using data from only one satellite. In these cases, the ion diffusion region moved relative to the spacecraft in such a way that the measurements showed a clear and rapid transition from outflow region signatures to inflow region signatures and back.

An example ion diffusion region encounter time interval (from encounter number 4 in Table 1) is shown in Fig. 2. Only data from spacecraft 1 and 4 are shown in the figure. Spacecraft 3 was situated some distance away from the other spacecraft in the negative $Z_{\mathrm{GSM}}$ direction and did not observe any of the outflow regions during most of the encounter. Spacecraft 2 does not provide any ion data and so data from that spacecraft is not included, for clarity. The panels in Fig. 2 show, from the top: the magnetic field X, Y and Z components, the ion velocity X component, the plasma beta, the anisotropy ($\frac{\text{aligned flux}-\text{perpendicular flux}}{\text{aligned flux}+\text{perpendicular flux}}$), the electron density derived from the spacecraft potential (Pedersen et al., 2008) (only the spacecraft 1 potential was within the criteria defined in Pedersen et al., 2008), the electric field Y component (0.02 s resolution) and in the bottom panel: the spacecraft 1 electric field Y component (black, 4 s resolution) and spacecraft 1 $(-v_{\mathrm{i}} \times B)_{\mathrm{y}}$ (green). The spacecraft 4 $(-v_{\mathrm{i}} \times B)_{\mathrm{y}}$ was found to be very close to zero during the entire interval, unlike the spacecraft 4 $E_{\mathrm{y}}$. For both spacecraft, the rough trend at this low time resolution shows $E + v_{\mathrm{i}} \times B \neq 0$ during most of the time interval, placing the spacecraft in the ion diffusion region. The observations in Fig. 2 have been divided into intervals A–F. A comparison of the data shown in Fig. 2 to the ion diffusion region encounter signature criteria

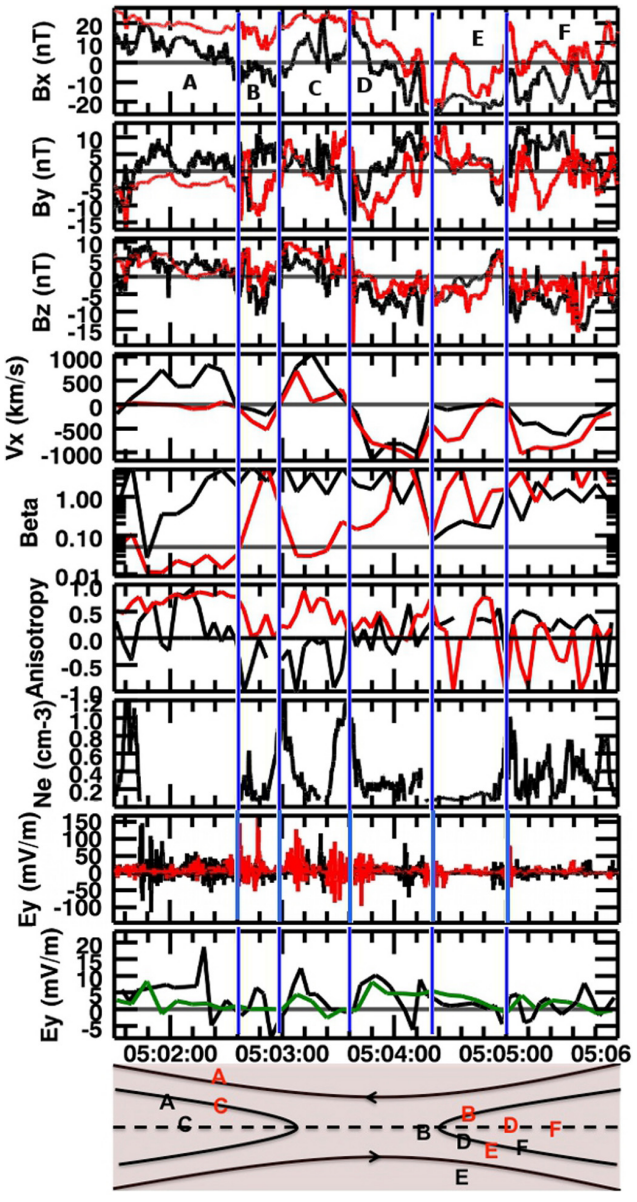


**Fig. 2.** Example of magnetic reconnection inflow and outflow time intervals observed by Cluster spacecraft 1 (black) and 4 (red) during the 15 September 2001 ion diffusion region encounter. The plots show (from the top panel): the magnetic field X, Y and Z components, the ion velocity X component, the plasma beta, the anisotropy $(\frac{\text{aligned flux}-\text{perpendicular flux}}{\text{aligned flux}+\text{perpendicular flux}})$, the electron density derived from the spacecraft potential (Pedersen et al., 2008) (only the spacecraft 1 potential was within the criteria defined in Pedersen et al. (2008)), the electric field Y component (0.02s resolution) and in the bottom panel: The SC1 electric field Y component (black, 4 s resolution) and SC1 $(-v_i \times B)_y$ (green). The observations have been divided into intervals A–F, identified as inflow/outflow intervals in the text. The bottom panel shows a rough sketch of the positions of spacecraft 1 (black letters) and spacecraft 4 (red letters) inside the ion diffusion region during intervals A–F (not to scale).

given above identified several outflow region time intervals observed by spacecraft 1 (interval A, C, D and F) and spacecraft 4 (interval B, C, D most of E, and F). The anisotropy during these outflow region observations vary from dominated by field aligned electron flux during interval A for spacecraft 1 and interval C for spacecraft 4 to dominated by perpendicular flux during interval C for spacecraft 1 and interval F for spacecraft 4. To identify the inflow region, we used the method described above, studying multi-spacecraft data. During interval A, ion outflow in the X direction was observed by spacecraft 1 but not by spacecraft 4. Looking at the magnetic field X component we note that spacecraft 4 was situated farther north of the current sheet than spacecraft 1. The spacecraft 4 plasma beta is lower than the plasma beta of spacecraft 1, in fact the spacecraft is probably entering the plasma sheet boundary layer or the lobe (beta less than 0.05). Assuming the ideal geometrical 2-D image of reconnection shown in Fig. 1, spacecraft 1 was observing the earthward outflow region while spacecraft 4 was situated in the Northern Hemisphere inflow region. In addition to the geometrical argument, spacecraft 4 was observing the inflow signatures: (1) there was no high velocity ion outflow, (2) the spacecraft was situated in the ion diffusion region and (3) the spacecraft did not cross the neutral sheet. There is no electron density data available but the high resolution electric field stays small until the end of interval A suggesting that (4) the spacecraft did not encounter the separatrix until possibly the end of the interval. A similar geometrical case could be made for most of interval E where at the same time spacecraft 4 observing a tailward outflow region while spacecraft 1 is observing inflow region signatures in the Southern Hemisphere. During this time interval, however, the difference in value between $E_y$ and $(-v_i \times B)_y$ is small, although the exact difference is difficult to pinpoint due to the the low time resolution. The anisotropy panel shows field aligned electron flux dominating both the inflow regions observed by the two spacecraft, but the effect is clearly strongest in the inflow region observed by spacecraft 4.

The bottom panel in Fig. 2 shows a rough sketch of the positions of spacecraft 1 (black letters) and 4 (red letters) inside the ion diffusion region of Fig. 1 during the intervals A–E. The sketch is not to scale. The figure demonstrates the complexity of the diffusion region encounters, where the ion diffusion region as a whole moves across the spacecraft during the intervals both in the X- and the Z-direction, as can be inferred by the change of polarity in both $B_x$ and $V_x$.

## 3 Electron pitch angle distribution

The simplest approach to studying the outflow and inflow electron pitch angle distribution would be to find, for each pitch angle bin, the median electron flux of all inflow and outflow interval data points and compare. If the electron flux in the inflow regions is more field aligned than the electron

flux in the outflow regions, the difference between the median electron flux at the $0° - 15°$ pitch angle bin(parallel to the magnetic field direction) and the pitch angle bins at around 90° (perpendicular to the magnetic field direction) should be greater for the inflow regions than for the outflow regions. The same should be true of the difference between the $165° - 180°$ (anti-parallel to the magnetic field direction) pitch angle bin and the $\sim 90°$ pitch angle bins. The pitch angle distribution of measured electron flux in the inflow region should look like the letter U, while the distribution in the outflow region should be closer to a horizontal line. The median was chosen over the average to avoid having a very small number of extremely high flux measurements (found in some of the outflow regions) skew the results.

Figure 3 shows the median inflow (green line) and median outflow (blue line) electron flux for each pitch angle bin for all energies and all ion diffusion region encounter time intervals at Cluster spacecraft 1 and 4 (a) and (b). The green and blue crosses show the first and third quartiles of the inflow and outflow electron flux distributions respectively. Quartiles divide a distribution into four equal groups, the median being the midpoint of the distribution. The median of each pitch angle bin has been normalized to the perpendicular ($75° - 90°$ and $90° - 105°$) pitch angle bins to clearly show the difference in flux between the pitch angles. Both figures show the median inflow flux for all ion diffusion region encounters and energies to be slightly more field aligned than the median outflow flux, most of the time. However, the interquartile ranges show that the distributions of inflow and outflow electron flux measurements are similar and also that compared to the spread in the distributions, the difference between the two medians is negligible.

The above simple approach includes all ion diffusion region encounter data and does not take into account differences between the individual events and also between electron energy levels. We therefore consider an alternative approach by first finding, for each individual ion diffusion region encounter, the difference between the normalized median inflow and outflow electron flux for each pitch angle bin. The median of these differences could then be determined for each pitch angle bin. This procedure will of course only give a rough indication of the trend. The result is presented in Fig. 4a–d for spacecraft 1 and 4 (black and red line, respectively). The black and red crosses represent the first and third quartiles of the distributions. The narrowing of the distributions in the perpendicular pitch angle bins is caused by the normalization. Panel (a) includes electron flux at all energy levels. In panels (b)–(d), electron flux at energy levels 70 eV–500 eV, 500 eV–5 keV and 5 keV–24 keV are shown. These energy intervals were chosen to single out the behavior of low and high energy electrons in particular and were found through a trial and error process. For spacecraft 1 the median difference between the inflow and the outflow electron flux, when all energy levels were included, was positive for pitch angles close to 0° and 180°. As in Fig. 3, this suggests that

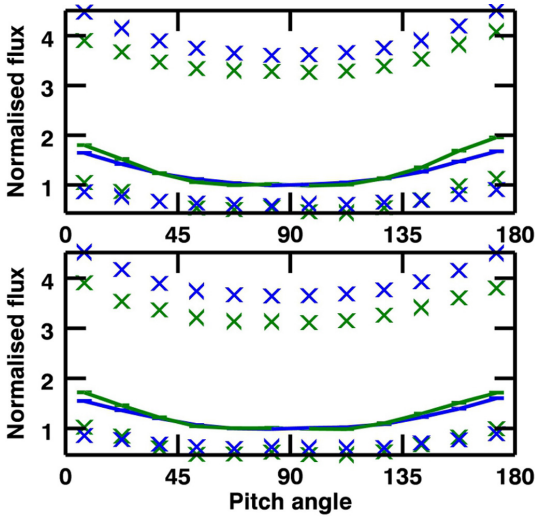


**Fig. 3.** Median electron differential energy flux for each of the 12 pitch angle bins, normalized to the average of the $75° - 90°$ and $90° - 105°$ pitch angle bins. Green line: Inflow region median, blue line: Outflow region median, green crosses: Inflow first and third quartiles, blue crosses: Outflow first and third quartiles. **(a)** Cluster spacecraft 1. **(b)** Cluster spacecraft 4.

the electron flux in the median inflow was slightly more field aligned than in the median outflow. The spacecraft 4 difference was closer to zero at 0° and slightly negative at 180°, suggesting a less clear picture. This result also holds at low energies in Fig. 4b but at medium energies 500 eV–5 keV in Fig. 4c there is a negative trend in the parallel pitch angles bins. At high energies 5 keV–24 keV the picture is similar to the low energy results, but with the spacecraft 4 median difference between the inflow and the outflow electron flux even closer to zero.

To fully explore the variation between the different ion diffusion region encounters, Figs. 5a and b show the spacecraft 1 normalized median inflow (green) and outflow (blue) electron flux for each event, at $0° - 30°$ (parallel) and $150° - 180°$ (anti-parallel) pitch angle. Because of the normalization, a value greater than 1 on the Y-axis implies a median electron flux greater than the median electron flux in the perpendicular bins. The numbers on the x-axis correspond to the numbered events (ion diffusion region encounters) in Table 1. The crosses represent the first and third quartiles of the inflow and outflow electron flux distributions. Figures 5c–d shows the same for spacecraft 4. For spacecraft 1, there were 14 ion diffusion region encounters where both the inflow and the outflow regions could be identified. For spacecraft 4, this number was 19. For many of the encountered ion diffusion regions the difference between normalized median inflow and outflow is small, but for a few ion diffusion regions the inflow region electron flux median is clearly more field aligned than the outflow region flux. Examples include events number 3, 4, 5, 9 and 16. The first and third quartile

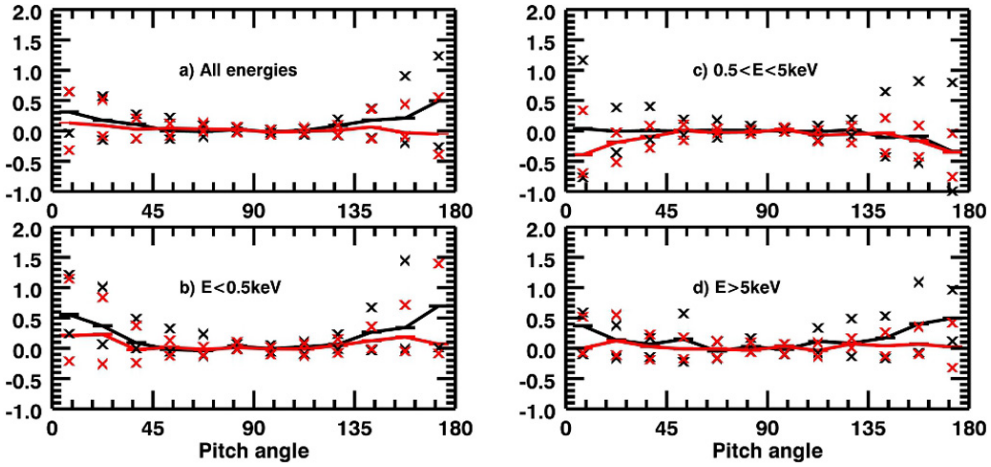


**Fig. 4.** Median difference between the normalized median inflow electron flux and the median outflow electron flux . All time intervals from all ion diffusion region encounters are included. Black line: Cluster spacecraft 1, red line: Cluster spacecraft 4. Crosses: first and third quartile of the distributions. **(a)** All energies, **(b)** electron energies 70 eV–500 eV, **(c)** electron energies 500 eV–5 keV, **(d)** electron energies 5 keV–24 keV.

marks show that in most cases, the bulk of the data points in the inflow electron flux distribution covers a narrower range than in the outflow distribution and also that the shape and range of the distributions vary considerably between ion diffusion regions.

The results shown in Fig. 5 suggest that there are in fact ion diffusion regions where the inflow electron flux is much more field aligned than the outflow flux (including ion diffusion region encounter number 5 in Table 1, on 1 October 2001, analyzed by Chen et al., 2008) but that this is not a consistent feature across all ion diffusion regions. An investigation of such plots at the energy ranges of Fig. 4b–d (not shown) reveals trends in the results similar to the ones in Fig. 4.

## 4 Discussion

Analyses of individual events observed by satellites, as well as simulations, have suggested that the electron flux in the inflow region is mostly field aligned in contrast with the electrons in the outflow region that have a flat-top isotropic distribution. In this multi-event study, the median behavior, considering all energies and ion diffusion region encounters, does show a trend of inflow region electron flux being slightly more field aligned than the outflow electron flux. However, there are differences not only between ion diffusion regions but also between energy ranges. Low and high energy electron flux is most field aligned in the inflow region in a majority of, but not all, ion diffusion region encounters. At medium energies (500 eV–5 keV) the trend is for a more field aligned outflow electron flux.

The large variation in field alignment between encountered ion diffusion regions may have many sources; real or produced by the data analysis and ion diffusion region selection. Identification of the inflow region can be difficult due to the relative nature of the method and as such the signatures are less clear cut than for the outflow regions. The difficulty in identifying these regions leads to fewer inflow region data points than outflow region data points. In addition, the inflow region data may be contaminated by data points from non-reconnection regions by simply being non-outflow regions rather than an inflow region. Another point to consider is the choice of the median to represent the electron flux distributions. As mentioned above, the choice of using the median rather than the mean was made to avoid having a small number of extremely high flux data points ($\sim$10 out of $\sim 10^4$ per affected pitch angle bin per reconnection event) skew the results. These data points were located in the outflow region distribution and mostly in the field aligned pitch angle bins. The median was consequently judged to provide the best representation of the bulk of the outflow region distribution.

There are many potential sources to real differences between ion diffusion regions. For example, areas within the outflow and inflow regions may have different degrees of electron flux field alignment, with areas close to the separatrix as a candidate for the most field aligned electron flux. Other differences between the encountered ion diffusion regions were identified and tested against the degree of field alignment in the inflow and outflow regions, such as the magnitude of the outflow region ion velocity, the magnitude of the total and component magnetic field in the area, the plasma beta, ion density and electron energy distribution within the ion diffusion regions. None of these factors seemed to play a significant or consistent role in the degree of field alignment in the inflow or outflow regions. A closer look at some of the ion diffusion region encounters also revealed that the electron pitch angle conditions in the inflow and outflow regions would change significantly within

ion diffusion regions as well, but whether this was a change that occurred over time or whether the spacecraft penetrated different areas of the inflow/outflow regions was difficult to establish.

Another factor that may contribute to the difference in inflow and outflow field alignment between events is whether the reconnection process is occurring on open (lobe) or closed (plasma sheet) magnetic field lines. The electrons in the inflow region of open field line reconnection are colder and expected to be less field aligned than the hotter inflow electrons of closed field line reconnection. It could follow that during closed field line reconnection processes, the difference in field alignment between the inflow and outflow electron flux is larger than during reconnection on open field lines. Six of the reconnection processes were found to occur on open magnetic field lines (events number 3, 4, 5, 9, 14 and 17). The temperature and plasma beta of the inflow region time intervals identified during these events were within the range of established lobe values (below 0.5 keV and 0.05, respectively) and the Alfvén speed in the outflow region time intervals was significantly higher than for the other events (order of magnitude $10^3$). A study of Fig. 5 shows that the electron flux in the inflow region is significantly more field aligned than in the outflow region during four of the six open field line events. The remaining two open field line events show the opposite result. There are also closed field line reconnection events (number 16 and 19) where the outflow region electron flux is more field aligned than the inflow flux and several others where the difference is small. Clearly there is no strong correlation between the difference in inflow and outflow field alignment and open/closed field line reconnection.

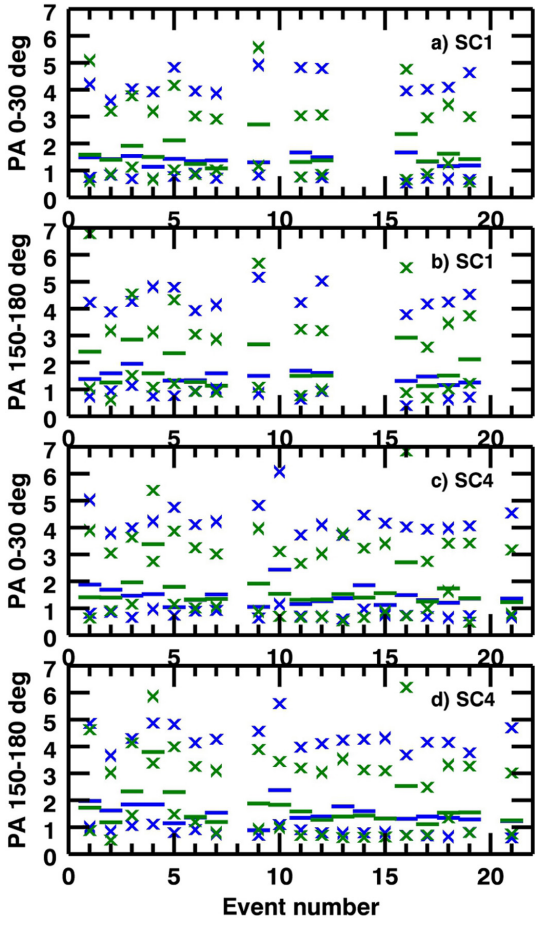


**Fig. 5.** Median normalized inflow electron flux (green lines) and outflow electron flux (blue lines) for each ion diffusion region encounter (see Table 1). A value greater than 1 means that the parallel/anti-parallel flux dominates over the perpendicular. Green crosses: inflow first and third quartiles, blue crosses: Outflow first and third quartiles. **(a)** Cluster spacecraft 1, $0° - 30°$ pitch angle bin (parallel). **(b)** Cluster spacecraft 1, $150° - 180°$ pitch angle bin (anti-parallel). **(c)** Cluster spacecraft 4, $0° - 30°$ pitch angle bin. **(d)** Cluster spacecraft 4, $150° - 180°$ pitch angle bin.

## 5 Summary

It has previously been reported that the electron flux in the magnetic reconnection inflow region is predominantly aligned with the magnetic field, while in the outflow region the bulk electron direction movement is more isotropic (Nagai et al., 2001; Egedal et al., 2005; Chen et al., 2008; Egedal et al., 2010). In this paper, we have tested the degree of electron field alignment in the outflow and inflow regions of 21 ion diffusion regions. The inflow and outflow regions were identified using the set of criteria given above. We demonstrate that while the bulk electron flux in the identified inflow regions are indeed more field aligned than the bulk flux in the outflow regions during some ion diffusion region encounters, the variation between ion diffusion regions and indeed within some ion diffusion region encounters is so large that it cannot be said to be a general feature of magnetic reconnection in the Earth's magnetotail. The reason for this variation is unknown and testing for correlation with factors such as the magnetic field magnitude, ion velocity, plasma beta, distribution of electron energies and the magnetic reconnection occurring on open or closed field lines has not yielded any clear answers.

It may be that our criteria used to define the ion diffusion region still allowed non diffusion regions to be analysed such that a broader region of the out and inflow regions was included. One key aspect in this is data resolution. All events were highly variable as presented above and one further result of this work is to highlight the requirement for much higher time resolution measurements to probe the electron diffusion region and unravel the topology of the reconnection process. This work will only be possible with the upcoming launch of MMS.

*Acknowledgements.* The authors would like to acknowledge the Cluster Active Archive and Cluster instrument teams, in particular

FGM, PEACE and CIS, for providing the data. JPE holds an STFC Advanced Fellowship at ICL.

Guest Editor A. Masson thanks A. Retinò and another anonymous referee for their help in evaluating this paper.

## References

Asano, Y., Nakamura, R., Shinohara, I., Fujimoto, M., Takada, T., Baumjohann, W., Owen, C. J., Fazakerley, A. N., Runov, A., Nagai, T., Lucek, E. A., and Rème, H.: Electron flat-top distributions around the magnetic reconnection region , J. Geophys. Res., 113, A01207, doi:10.1029/2007JA012461, 2008.

Balogh, A., Carr, C. M., Acuña, M. H., Dunlop, M. W., Beek, T. J., Brown, P., Fornacon, K.-H., Georgescu, E., Glassmeier, K.-H., Harris, J., Musmann, G., Oddy, T., and Schwingenschuh, K.: The Cluster Magnetic Field Investigation: overview of in-flight performance and initial results, Ann. Geophys., 19, 1207–1217, doi:10.5194/angeo-19-1207-2001, 2001.

Borg, A. L.: A study of magnetic reconnection events observed by the Cluster satellites in the Earth's magnetotail, Ph.D. thesis, Univ. of Oslo, Oslo, Norway, 2006.

Borg, A. L., Øieroset, M., Phan, T. D., Mozer, F. S., Pedersen, A., Mouikis, C., McFadden, J. P., Twitty, C., Balogh, A., and Rème, H.: Cluster encounter of a magnetic reconnection diffusion region in the near-Earth magnetotail on September 19, 2003, Geophys. Res. Lett., 32, L19105, doi:10.1029/2005GL023794, 2005.

Chen, L. J., Bessho, N., Lefebvre, B., Vaith, H., Fazakerley, A., Bhattacharjee, A., Puhl-Quinn, P. A., Runov, A., Khotyaintsev, Y., Vaivads, A., Georgescu, E., and Torbert, R.: Evidence of an extended electron current sheet and its neighboring magnetic island during magnetotail reconnection, J. Geophys. Res., 113, A12213, doi:10.1029/2008JA013385, 2008.

Eastwood, J. P., Phan, T. D., Øieroset, M., and Shay, M. A.: Average properties of the magnetic reconnection ion diffusion region in the Earth's magnetotail: The 2001-2005 Cluster observations and comparison with simulations, J. Geophys. Res., 115, A08215, doi:10.1029/2009JA014962, 2010.

Egedal, J., Øieroset, M., Fox, W., and Lin, R. P.: In situ discovery of an electrostatic potential, trapping electrons and mediating fast reconnection in the Earth's magnetotail, Phys. Rev. Lett., 94, 025006, doi:10.1103/PhysRevLett.94.025006, 2005.

Egedal, J., Lê, A., Katz, N., Chen, L. J., Lefebvre, B., Daughton, W., and Fazakerley, A.: Cluster observations of bidirectional beams caused by electron trapping during antiparallel reconnection, J. Geophys. Res., 115, A03214, doi:10.1029/2009JA014650, 2010.

Fujimoto, M., Nakamura, M. S. , Shinohara, I., Nagai, T., Mukai, T., Saito, Y., Yamamoto T., and Kokubun, S.: Observations of earthward streaming electrons at the trailing boundary of a plasmoid, Geophys. Res. Lett., 24, 2893–2896, 1997.

Giovanelli, R. G.: A theory of chromospheric flares, Nature, 158, 81–82, 1946.

Johnstone, A. D., Alsop, C., Burge, S., Carter, P. J., Coates, A. J., Coker, A. J., Fazakerley, A. N., Grande, M., Gowen, R. A., Gurgiolo, C., Hancock, B. K., Narheim, B., Preece, A., Sheather, P. H., Winningham, J. D., and Woodliffe, R. D: PEACE: A plasma electron and current experiment, Space Sci. Rev., 79, 351–398, 1997.

Khotyaintsev, Yu. V., Vaivads, A. , Retinò, A., Andre, M., Owen, C. J., and Nilsson, H.: Formation of Inner Structure of a Reconnection Separatrix Region, Phys. Rev. Lett., 97, 205003, doi:10.1103/PhysRevLett.97.205003, 2006.

Laakso, H, Perry, C., McCaffrey, S., Herment, D., Allen, A. J., Harvey, C. C., Escoubet, C. P., Gruenberger, C., Taylor, M. G. G. T., and Turner, R.: Cluster Active Archive: Overview, 3–37, The Cluster Active Archive, Astrophysics and Space Science Proceedings, edited by: Laakso, H., Taylor, M. G. G. T., and Escoubet, C. P., Springer, 2010.

Le, A., Egedal, J., Fox, W., Katz, N., Vrublevskis, A., Daughton, W., and Drake, J. F.: Equations of state in collisionless magnetic reconnection, Phys. Plasmas, 17, 055703, doi:10.1063/1.3309425, 2010.

Nagai, T.: Location of Magnetic Reconnection in the magnetotail, Space Sci. Rev., 122, 39–54, doi:10.1007/s11214-006-6216-4, 2006.

Nagai, T., Shinohara, I., Fujimoto, M., Hoshino, M., Saito, Y., Machida, S., and Mukai, T.: Geotail observations of the hall current system: Evidence of magnetic reconnection in the magnetotail, J. Geophys. Res., 106, 25929–25949, 2001.

Øieroset, M., Phan, T. D., Fujimoto, M., Lin, R. P., and Lepping, R. P.: In situ detection of collisionless reconnection in the Earth's magnetotail, Nature, 412, 414–417, 2001.

Pedersen, A., Lybekk, B., André, M., Eriksson, A., Masson, A., Mozer, F. S., Lindqvist, P.-A., Décréau, P. M. E., Dandouras, I., Sauvaud, J.-A., Fazakerley, A., Taylor, M. G. G. T., Paschmann, G., Svenes, K. R., Torkar, K., and Whipple, E.: Electron density estimations derived from spacecraft potential measurements on Cluster in tenuous plasma regions, J. Geophys. Res., 113, A07S33, doi:10.1029/2007JA012636, 2008.

Rème, H., Aoustin, C., Bosqued, J. M., Dandouras, I., Lavraud, B., Sauvaud, J. A., Barthe, A., Bouyssou, J., Camus, Th., Coeur-Joly, O., Cros, A., Cuvilo, J., Ducay, F., Garbarowitz, Y., Medale, J. L., Penou, E., Perrier, H., Romefort, D., Rouzaud, J., Vallat, C., Alcaydé, D., Jacquey, C., Mazelle, C., d'Uston, C., Möbius, E., Kistler, L. M., Crocker, K., Granoff, M., Mouikis, C., Popecki, M., Vosbury, M., Klecker, B., Hovestadt, D., Kucharek, H., Kuenneth, E., Paschmann, G., Scholer, M., Sckopke, N., Seidenschwang, E., Carlson, C. W., Curtis, D. W., Ingraham, C., Lin, R. P., McFadden, J. P., Parks, G. K., Phan, T., Formisano, V., Amata, E., Bavassano-Cattaneo, M. B., Baldetti, P., Bruno, R., Chionchio, G., Di Lellis, A., Marcucci, M. F., Pallocchia, G., Korth, A., Daly, P. W., Graeve, B., Rosenbauer, H., Vasyliunas, V., McCarthy, M., Wilber, M., Eliasson, L., Lundin, R., Olsen, S., Shelley, E. G., Fuselier, S., Ghielmetti, A. G., Lennartsson, W., Escoubet, C. P., Balsiger, H., Friedel, R., Cao, J.-B., Kovrazhkin, R. A., Papamastorakis, I., Pellat, R., Scudder, J., and Sonnerup, B.: First multispacecraft ion measurements in and near the Earths magnetosphere with the identical Cluster ion spectrometry (CIS) experiment, Ann. Geophys., 19, 1303–1354, doi:10.5194/angeo-19-1303-2001, 2001.

Retinò, A., Vaivads, A., André, M., Sahraoui, F., Khotyaintsev, Y., Pickett, J. S., Bavassano Cattaneo, M. B., Marcucci, M. F., Morooka, M., Owen, C. J., Buchert, S. C., and Cornilleau-Wehrlin, N.: Structure of the separatrix region close to a magnetic reconnection X-line: Cluster observations, Geophys. Res. Lett., 33, L06101, doi:10.1029/2005GL024650, 2006.

Slavin, J. A., Lepping, R. P., Gjerloev, J., Fairfield, D. H., Hesse,

M., Owen, C. J., Moldwin, M. B., Nagai, T., Ieda, A., and Mukai, T.: Geotail observations of magnetic flux ropes in the plasma sheet, J. Geophys. Res., 108, 1015, doi:10.1029/2002JA009557, 2003.

Vasyliunas, V. M.: Theoretical models of magnetic field line merging, Rev. Geophys., 13, 303–336, doi:10.1029/RG013i001p00303, 1975.